

Chromatism compensation of the PETAL multipetawatt high-energy laser

Jérôme Neauport, N Blanchot, C Rouyer, C Sauteret

► **To cite this version:**

Jérôme Neauport, N Blanchot, C Rouyer, C Sauteret. Chromatism compensation of the PETAL multipetawatt high-energy laser. *Journal of Optics A: Pure and Applied Optics*, IOP Publishing, 2007, 10.1364/AO.46.001568 . cea-01217058

HAL Id: cea-01217058

<https://hal-cea.archives-ouvertes.fr/cea-01217058>

Submitted on 18 Oct 2015

HAL is a multi-disciplinary open access archive for the deposit and dissemination of scientific research documents, whether they are published or not. The documents may come from teaching and research institutions in France or abroad, or from public or private research centers.

L'archive ouverte pluridisciplinaire **HAL**, est destinée au dépôt et à la diffusion de documents scientifiques de niveau recherche, publiés ou non, émanant des établissements d'enseignement et de recherche français ou étrangers, des laboratoires publics ou privés.

Chromatism compensation of the PETAL multipetawatt high-energy laser

J. Néauport, N. Blanchot, C. Rouyer, and C. Sauteret

High-energy petawatt lasers use series of spatial filters in their amplification section. The refractive lenses employed introduce longitudinal chromatism that can spatially and temporally distort the ultrafast laser beam after focusing. To ensure optimum performances of petawatt laser facilities, these distortions need to be corrected. Several solutions using reflective, refractive, or diffractive optical components can be addressed. We give herein a review of these various possibilities with their application to the PETAL (Petawatt Aquitaine Laser at the Laser Integration Line facility) laser beamline and show that diffractive-based corrections appear to be the most promising. © 2007 Optical Society of America
OCIS codes: 140.7090, 050.5080.

1. Introduction

The past decade has seen the development of numbers of ultrahigh-energy laser facilities driven by fast ignition and inertial confinement fusion application advances.¹ High-energy petawatt projects like Omega-Extended Performance² (Laboratory for Laser Energetics, University of Rochester, USA), National Ignition Facility (NIF) Petawatt Laser³ (Lawrence Livermore National Laboratory, USA), PICO2000⁴ petawatt laser (Laboratoire pour l'Utilisation des Lasers Intenses, France), Vulcan Petawatt Laser⁵ (Rutherford Appleton Laboratory, UK), Petawatt Aquitaine Laser (PETAL)⁶ (Commissariat à l'Énergie Atomique, France), and the Fast Ignition Realization Experiment (FIREX)⁷ (Institute of Laser Engineering, Japan) will allow unique experiments in the field of ultrahigh intensity sciences, extreme plasma physics, astrophysics, radiography, and demonstration of fast ignition by combination of petawatt or multipetawatt, kilojoule beams and nanosecond multikilojoule beams. In all these laser systems, amplifiers are separated by large spatial filters. These spatial fil-

ters, using a pair of refractive lenses, are used to clean the beam of unwanted intensity modulations at high spatial frequencies⁸ and also to extend and/or to image the spatial profile on each amplifier stages. In single-pass amplifier systems, spatial filters are passed once, while in multipass amplifier configurations, spatial filters can be passed two to four times, depending on the choice of architecture. Because of the dependence of the glass index with wavelength, in traversing of a refractive lens a polychromatic light is focused in multiple foci along the lens axis, each corresponding to a given wavelength. This aberration is known as longitudinal chromatic aberration⁹ and is additive. For spatial filters, this effect ensures that only the central wavelength is collimated while the other wavelengths acquire a divergence or a convergence. For long-pulse laser systems such as NIF¹⁰ or Laser Megajoule (LMJ)¹¹, this effect can be neglected. But for short pulses, i.e., of large spectral bandwidth, this chromatic aberration can significantly distort temporally and spatially the beam in the focal plane. This phenomenon has been previously described by Bor¹² and needs to be corrected for most of the petawatt class laser facilities.

Many solutions exist to correct the longitudinal chromatism of spatial filters lenses; they were subsequently studied in the field of short pulses,¹³ microscopy,¹⁴ or lens design for visible wavelength.¹⁵ The most classical method consists of employing achromatic doublets made of two different glasses.⁹ Another solution based on the same principle is to replace some plane mirrors by an adequate coupling of a diverging lens and a spherical mirror. One can also take advantage of the inverse chromatic aberration

J. Néauport (jerome.neauport@cea.fr), N. Blanchot, and C. Rouyer are with the Commissariat à l'énergie atomique, Centre d'études scientifiques et techniques d'Aquitaine, B.P. 2, 33114 Le Barp, France. C. Sauteret is with the Laboratoire pour l'Utilisation des Lasers Intenses, Ecole Polytechnique, Unité mixte de Recherche 7605, 91128 Palaiseau, France.

Received 6 September 2006; revised 9 November 2006; accepted 29 November 2006; posted 1 December 2006 (Doc. ID 74766); published 1 March 2007.

0003-6935/07/091568-07\$15.00/0

© 2007 Optical Society of America

tion of a diffractive optic such as a grating or a Fresnel zone plate.^{16–18} Last, it is also possible to design a null power triplet compensating the chromatic aberration.

This paper is divided in three parts. The amplifier section of the PETAL facility is depicted in Section 2 with details of the chromatic aberration to be corrected. We then review the various compensation solutions with their feasibility in our facility. Section 3 is thus devoted to the analysis of correcting solution using glasses of various types based on the achromatic doublet principle. Section 4 focuses on the use of diffractive optics for chromatism correction.

2. Petawatt Aquitaine Laser Amplifier Section

The PETAL facility is designed to deliver 3.6 kJ of energy in 500 fs at the wavelength of 1.053 μm and is an additional short pulse beam to the Laser Integration Line (LIL)¹¹ facility. The PETAL amplifier section has the same architecture as the LIL/LMJ amplifier section¹⁹ using a single 400 mm \times 400 mm beam. It is a four-pass system with angular multiplexing and an L-turn (see Fig. 1). It uses 16 amplifier laser slabs arranged in two sets. The front-end pulse (up to 100 millijoules) is injected in the transport spatial filter (FST), passes into amplifier groups, bounces on the M1 deformable mirror, and passes a

second time in the 16 slabs. The beam is reflected off Mdt1 into the L-turn, reflects on the M2 mirror, and goes back on M1 and then exits the amplifier section after L4, the last lens of FST. It is then sent to the transport section and focused after compression²⁰ with a parabola into the center of the vacuum chamber.

The delay introduced by a single lens can be expressed as²¹

$$\Delta T = \frac{\lambda r^2}{2cf(n-1)} \frac{dn}{d\lambda} = -\frac{\lambda r^2}{2cf^2} \frac{df}{d\lambda}, \quad (1)$$

where f is the focal length of the lens, λ is the central wavelength, n is the refractive index of glass, c is the velocity of light, and r is the distance of the marginal ray from the axis.

If we now consider a series of spatial filters consisting of N lenses, the effect is additive, and the total delay becomes

$$\Delta T = \sum_{i=1}^N \frac{\lambda r_i^2}{2cf_i(n_i-1)} \left(\frac{dn}{d\lambda} \right)_i. \quad (2)$$

After final focusing with a reflective parabola of focal length F and half-diameter r , this total pulse delay

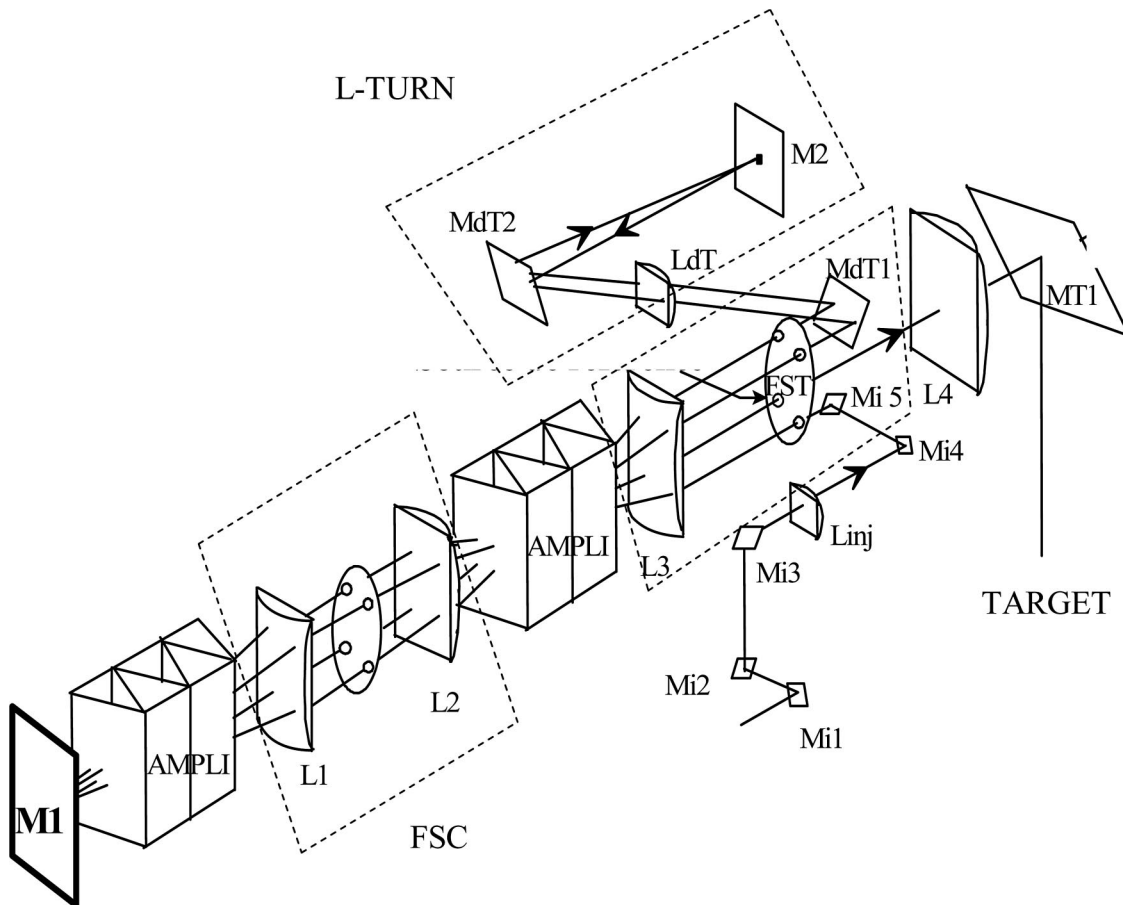


Fig. 1. PETAL amplifier section baseline with angular multiplexing. The L-turn is realized with two mirrors (Mdt2, M2). The transport spatial filter (FST) and cavity spatial filter (FSC) are surrounded.

Table 1. Delay Contribution of Each Lens of the Petawatt Aquitaine Laser Amplifier Section

Lens	Focal Length (mm)	Half-Diameter (mm)	Delay (fs)	Number of Passes	Total Delay (fs)
Linj	2765	18.76	6	1	6
L3	26282	178.32	58	4	231
L2	9972	178.32	152	4	608
L1	9791	175.08	149	4	597
Ldt	5000	33.92	11	2	22
L4	26282	178.32	58	1	58

corresponds to the following focal shift [Eq. (3)], where f_i and δf_i are the focal length and focal shift of lens i .

$$\Delta F(\lambda) = \frac{F^2}{r^2} \sum_{i=1}^N \frac{r_i^2}{f_i} \left[\frac{\delta f_i(\lambda)}{f_i} \right] = \frac{F^2}{r^2} \times \frac{(\lambda - \lambda_0)}{\lambda_0} \times 2c \times \Delta T. \quad (3)$$

The focal shift divided by the Rayleigh distance to the target is therefore proportional to the cumulated delay of the marginal ray divided by the pulse duration,

$$\frac{\Delta F}{Z} = K \times \frac{\Delta T}{\tau}. \quad (4)$$

Here Z is the Rayleigh distance on the target, τ is the pulse duration, and K is a form factor equal to 8 for a Gaussian beam with a Gaussian spectrum.

In the case of our PETAL amplifier section, all lenses are made of fused silica (Corning 7980). The index is $n = 1.449$ and $dn/d\lambda = -1.22 \times 10^{-5} \text{ nm}^{-1}$ at the wavelength of $1.053 \mu\text{m}$. Table 1 summarized the delay contribution of each lens of our amplifier section. Overall, due to large component size, a total delay of 1520 fs is introduced in traversing the lenses of our system. This quantity at the edge of the square beam is almost three times the expected duration of the PETAL laser pulse and reaches four times this pulse duration for the corner of the square beam. Numerical simulations⁶ have shown that both temporal and spatial distortions are combined and induce a decrease of the peak intensity on target by a factor of 8 compared to the ideal case (no chromatism). Consequently, a chromatism compensator has to be implemented in the laser system.

3. Reflective-Refractive-Based Chromatism Corrections

Wavelength dependence of the refractive index of a given glass is usually expressed by glass manufacturers by its Abbé number ν [see Eq. (5)], where n_D , n_F , and n_C are the indices for the three visible emission rays of sodium and hydrogen (589.3 nm, 486.1 nm, and 656.3 nm, respectively)²²:

$$\nu = \frac{n_D - 1}{n_F - n_C}. \quad (5)$$

This Abbé number is suitable for correction to be made in the visible range. First-order chromatism compensation then takes benefits of the existence of two main family of glasses called flint glass (low index and high Abbé number) and crown glass (high index and low Abbé number). Adequate combination of these glasses can be used to compensate chromatic aberration.

Transposition of this principle to high-power laser facilities operating at $1.053 \mu\text{m}$ must take into account several additional criteria or constraints:

- Glass must be chosen based on its index n and wavelength dependence $dn/d\lambda$ at 1.053 nm . For the PETAL facility a typical spectrum of 3 nm is used in the amplifier section.
- Glass must exhibit a high damage threshold. Typical values of a few J/cm^2 to $20 \text{ J}/\text{cm}^2$ at $1.053 \mu\text{m}$ for 3 ns pulses are to be considered at the PETAL facility depending on the lens to be corrected in the amplifier section.
- Glass must exhibit a low nonlinear index n_2 to limit the B -integral to a value that avoids any self-focusing phenomenon^{8,23} and compressed pulse profile distortions.
- Glass must be feasible in rather large size (see Table 1 for PETAL lenses) and with a high refractive-index homogeneity and transparency at $1.053 \mu\text{m}$.

Most of these data can be found in the glass manufacturers catalog (Hoya, Corning, Schott, or others); we based our calculation on and referenced our glasses to the Schott optical glass catalog.²⁴ Laser-induced damage threshold values could be found in work from Hack *et al.*²⁵ Authors made an extensive study of the damage threshold at the wavelength of $1.064 \mu\text{m}$ for pulses duration of 3 ns of many different optical glasses and detailed some nonlinear index values as well. Additional data regarding nonlinear index could also be found in Adair *et al.*²⁶ Let us now consider a correction with a first lens made of fused-silica 7980 from Corning (equivalent to the crown glass described above); then the flint glass could be, for example, LF5 or LLF-1 Schott glass. For LF-5, we have $n = 1.556$, $dn/d\lambda = -1.69 \times 10^{-5} \text{ nm}^{-1}$, and $n_2 = 2.73 \times 10^{-13} \text{ e.s.u}$ at the wavelength of $1.053 \mu\text{m}$, equivalent⁸ to $\gamma = 7.35 \times 10^{-16} \text{ cm}^2/\text{W}$. Most of the high-index homogeneity optical glasses are not available at sizes of more than $180 \text{ mm} \times 180 \text{ mm}$. Moreover, platinum inclusions can be a major issue for operation on high-power laser facilities. Significant efforts can be made to limit the number and size of these inclusions while preserving high-index homogeneity for specific large productions²⁷; in our case this was not economically viable. Therefore, refractive correction is limited to a part with a section of less than $180 \text{ mm} \times 180 \text{ mm}$.

A. Achromats

The simplest method to correct chromatism of a single thin lens is to replace it by an achromat made of two thin lenses in contact made of two different

glasses. As explained before, for PETAL, this correction is practically limited to the injection lens L_{inj} and L-turn lens L_{dt} due to size availability considerations. The L_{dt} fused-silica lens with a focal point of 5 m can be replaced by an achromatic doublet with a fused-silica converging lens and a LF5 diverging lens with the following surface radii, $R_1 = 0.46$ m, $R = +0.5$ m, and $R_2 = -0.98$ m, for example ($R > 0$ for convex). Because it is limited to L_{inj} and L_{dt} , Table 1 shows that a delay of only 28 fs can be compensated with this technique, which is insufficient.

B. Plane Mirror Substitution by an Equivalent Diverging Lens and Concave Mirror Combination

Alternatively, one can also benefit from the inverse chromatism of a diverging lens by replacing a plane mirror by an equivalent combination of a concave spherical mirror and diverging lens²⁸ (see Fig. 2). For the PETAL amplifier section, it can be done by changing the L-turn mirror M2 by this optical system. The beam half-section on the M2 mirror is 33.92 mm. The induced delay is then calculated with Eq. (1). Trying to compensate the whole 1520 fs delay of our system with this combination leads to a LF5 diverging lens of focal length $f = -80.8$ mm. Good transmitted wavefront quality of an almost $f/1$ lens can be difficult to achieve, in particular for modulations at mid spatial frequencies where strict specifications are needed for these types of laser facilities.²⁹

Regarding the B -integral, the nonlinear index of LF5 is three times bigger than the nonlinear index of fused silica. Therefore the Kerr effect induced by the double pass in the LF5 compensation lens will lead to an increase of the B -integral of the system. This contribution ΔB is given by the equation $\Delta B = 2 \times (2\pi/\lambda) \times \gamma \times I \times e$ with typical values of the thickness $e = 1$ cm and intensity of $I = 4.10^8$ W/cm². The obtained B -integral contribution of $\Delta B = 3.5 \times 10^{-2}$ radians can consequently be neglected, showing that nonlinear contribution is not an issue in this case. Let us outline that the contribution of the corrector diverging element to the B integral could be minimized by using calcium fluoride instead of LF5 optical glass. But since calcium fluoride³⁰ has a $dn/d\lambda$ of approximately -6×10^{-6} nm⁻¹ around 1 μ m, i.e., three times less than LF5, it would lead to a nonmanufac-

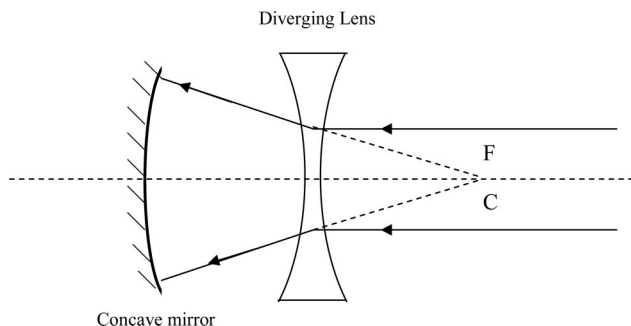


Fig. 2. Optical system equivalent to a plane mirror. Curvature center of mirror C and lens focus point F are placed at the same position.

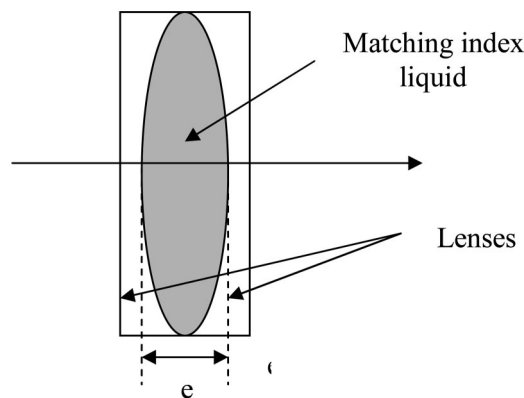


Fig. 3. Null power compensation system. Two plano-concave lenses with interspace filled with matching-index liquid of the same index as the lenses.

turable lens or to a possible delay compensation of a third of our total delay. Based on lens manufacturing difficulties, this correction principle cannot be retained for the PETAL laser facility.

C. Null Power Compensation System

The principle of this compensation null power system is to use two plano-concave lenses of the same radius with their spherical surfaces facing each other (see Fig. 3). A matching index liquid is then placed between the two spherical surfaces. Lenses and matching-index liquid are chosen to have the same index around 1 μ m. If e is the distance difference between marginal and on-axis rays in the liquid, the delay introduced by this combination is given by

$$\Delta T = \frac{\lambda}{c} \left[\left(\frac{dn}{d\lambda} \right)_{\text{glass}} - \left(\frac{dn}{d\lambda} \right)_{\text{liq}} \right] \times e, \quad (6)$$

where $(dn/d\lambda)_{\text{glass}}$ and $(dn/d\lambda)_{\text{liq}}$ denote the dependence of index of glass and matching-index liquid versus wavelength.

For a configuration with two fused-silica lenses and a Cargille code 6530³¹ matching-index liquid, we obtain a maximal delay compensation of 165 fs for $e = 10$ mm, equivalent to $f/3$ lenses for a system implemented in the L-turn. This delay compensation is insufficient to be used in our PETAL system. Moreover, uncertainty exists on the optical quality in transmission of such liquids and on their nonlinear index. In consequence, this solution was abandoned.

4. Diffractive-Based Chromatism Corrections

A. Principle

Holograms such as diffraction gratings have been widely used for achromatization since they exhibit an inverse chromatism compared to transparent materials. Modern optical design often benefits from this behavior.¹⁵⁻¹⁸

Let us consider a focusing grating of focal length f (see Fig. 4). In the first diffracted order, $\sin \alpha(r, \lambda) = N(r) \times \lambda$, where $N(r)$ is the line density of the grating

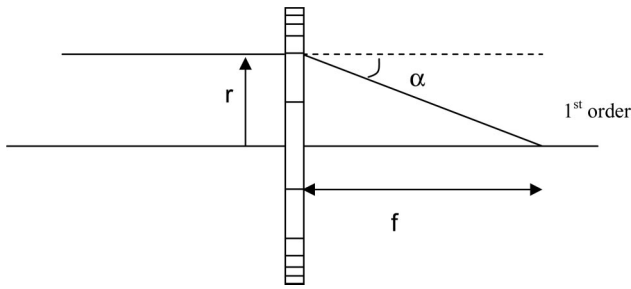


Fig. 4. Focusing grating.

at the marginal ray r . In the paraxial approximation, $f = r/\alpha = r/N(r) \times \lambda$. Therefore chromatic aberration of the grating can be expressed as

$$\frac{df}{d\lambda} = -\frac{f}{\lambda}. \quad (7)$$

Bor demonstrated²¹ that part two of Eq. (1) stays valid in the case of a Fresnel zone plate, and it can be extended as well to our focusing grating operating in its first order. Therefore the delay introduced by the grating can be expressed by combining Eqs. (1) and (7):

$$\Delta T = -\frac{\lambda r^2}{2cf^2} \frac{df}{d\lambda} = \frac{r^2}{2cf} = \frac{rN\lambda}{2c}. \quad (8)$$

By another way, Fig. 5 shows that this delay ΔT can be directly obtained by the difference between the marginal ray length and the axial ray length, $r^2/(2f)$.

The groove density of the grating for a ray having a distance h from the optic axis is expressed by the relation $N(h) = h/\lambda f$. When the ray is translated along the pupil periphery, it covers the m th groove. After passing a unique groove of a grating, the wave takes a delay of a period of the wave, i.e., λ/c . Thus, if m grooves of the grating are seen by the wave, the delay is, thanks to the quadratic variation of the line density of the focusing grating, expressed as

$$\Delta T = m \frac{\lambda}{c} = \frac{r^2}{2f\lambda} \times \frac{\lambda}{c} = \frac{rN\lambda}{2c}. \quad (9)$$

The number m of grooves therefore appears independent of the diffractive corrector characteristics, such as focal length or aperture diameter. Typically, to

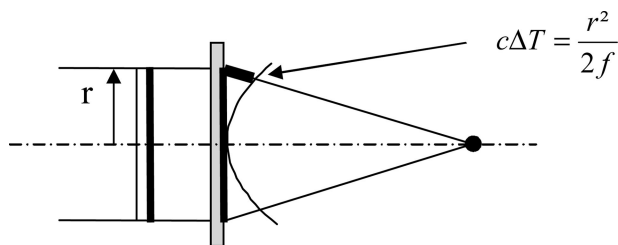


Fig. 5. Delay ΔT corresponds to the difference of the marginal and axial ray lengths.

compensate the 1520 fs delay of the PETAL facility, the diffractive corrector will have m grooves, with m equal to

$$m = \frac{c \times \Delta T}{\lambda} = 433 \text{ grooves}. \quad (10)$$

Application of the principle of this diffractive chromatic aberration can be done in the case of our PETAL facility by replacing, for example, the L-turn mirror M2 by an equivalent combination of a converging diffractive lens and convex spherical mirror on the equivalent baseline of Subsection 3.B. Equation (8) gives the focal length of the diverging element. For $r = 33.92$ mm on the M2 mirror, we find a focal length of $f = 2.523$ m. This corresponds to a line density of $N = 12.767$ lines/mm. Such a low line-density grating would exhibit very low diffraction efficiency. Thus in our high-power laser application, diffractive Fresnel lenses³² are preferred. It consists of a Fresnel lens with a binarized one-wave-deep profile. Using a four-mask manufacturing process, the 16 level diffractive Fresnel lenses can exhibit a theoretical diffraction efficiency of 98.5%.

We therefore see that our whole 1520 fs compensation can be made by a Fresnel convergent diffracting 16 level lens placed in our L-turn with a line density on the marginal ray of 12.767 lines/mm. Other difficulties shall be addressed with this peculiar component, such as wavefront quality in both mid and high frequencies¹⁸ and ghost beams due to the diffractive nature of the device. Damage threshold shall not be an issue since a bare fused-silica part is used. These specific points will be addressed in a future work.

B. Second-Order Chromatism Correction

The chromatic aberration compensation calculated in the previous subsections assumes that dependence of the index versus wavelength is linear. When this linear contribution is corrected, a nonlinear contribution called the second-order chromatism still remains. The quantitative effect of the second-order chromatism is estimated in this paragraph.

We herein assume that the chromatic “linear” aberration is compensated in our PETAL baseline by adding a Fresnel diffractive lens such as depicted in Subsection 4.A. Second-order chromatism of the diffractive compensator can be expressed by derivation of Eq. (7) at the second order:

$$\frac{d^2f}{d\lambda^2} = \frac{2f}{\lambda^2}. \quad (11)$$

Expanding the wavelength dependent of the focal length, we have

$$\left(\frac{\delta f}{f}\right)_{\text{dif}} = -\frac{\Delta\lambda}{\lambda} + \frac{\Delta\lambda^2}{\lambda^2} + O\left[\left(\frac{\Delta\lambda}{\lambda}\right)^3\right]. \quad (12)$$

For the refractive lenses, we have with the same way,

$$\left(\frac{\delta f}{f}\right)_{\text{ref}} = -\frac{\Delta\lambda}{(n-1)} \frac{dn}{d\lambda} + \left[\frac{1}{(n-1)^2} \left(\frac{dn}{d\lambda}\right)^2 - \frac{1}{2(n-1)} \frac{d^2n}{d\lambda^2} \right] \Delta\lambda^2 + O\left[\left(\frac{\Delta\lambda}{\lambda}\right)^3\right]. \quad (13)$$

The longitudinal chromatism Δz relative to the Rayleigh distance Z can be expressed thanks to Eq. (3) and with separation of refractive and diffractive contribution by

$$\frac{\Delta z}{Z} = \frac{1}{\lambda} \left\{ \left[\sum_{i=1}^P \frac{r_i^2}{f_i} \left(\frac{\delta f_i(\lambda)}{f_i}\right) \right]_{\text{ref}} + \left[\sum_{j=1}^M \frac{r_j^2}{f_j} \left(\frac{\delta f_j(\lambda)}{f_j}\right) \right]_{\text{dif}} \right\}. \quad (14)$$

Combination of Eqs. (12), (13), and (14) and annulations of the first-order term in $\Delta\lambda$ achieved by the first-order correction gives the following relations:

$$\frac{\Delta z}{Z} = \frac{\Delta\lambda^2}{\lambda^2} \left(\sum_{j=1}^M \frac{r_j^2}{f_j} \right)_{\text{dif}} \left[\frac{1}{\lambda} + \left(\frac{d^2n/d\lambda^2}{2dn/d\lambda} - \frac{1}{n-1} \frac{dn}{d\lambda} \right) \right]. \quad (15)$$

For our correction of Subsection 4.B with a diffractive Fresnel of focal length $f = 2.523$ m and radius $r = 33.92$ mm, a spectrum of $\Delta\lambda = 3$ nm, we have $\Delta z/Z = 4.4 \times 10^{-3}$. This second-order chromatism can thus be neglected.

5. Conclusions

Without any correction, the PETAL high-energy petawatt laser beam presents a chromatism that can reduce the intensity on target by a factor of 8. We have therefore reviewed various types of chromatic aberration corrections for their application to this facility. We have shown that, for compensation of the 1520 fs pulse broadening, refractive-based solutions offered low interest and small amount of time compensation. Moreover, high nonlinear index and small size availability of the optical glass to be used induced many constraints. Diffractive compensation solutions appear to be the most adequate solution. We have thus demonstrated that only one Fresnel diverging diffractive lens can be used for the compensation of the whole chromatism of our amplifier section. In this case, the second-order chromatism is negligible. Consequently, this diffractive correction principle is retained in the baseline of PETAL. Efforts are now made to check position of ghost beams and to make some experimental validations of a diffractive Fresnel lens manufactured from the calculation herein detailed.

This work is supported by the Conseil Régional d'Aquitaine and is performed under the auspices of the Institut Lasers et Plasmas.

References

1. J. D. Zuegel, S. Borneis, C. Barty, B. Le Garrec, C. Danson, N. Miyanaga, P. K. Rambo, C. Le Blanc, T. J. Kessler, A. W. Schmid, L. J. Waxer, J. H. Kelly, B. Kruschwitz, R. Jungquist,

- E. Moses, J. Britten, I. Jovanovic, J. Dawson, and N. Blanchot, "Laser challenges for fast ignition," in special issue on fast ignition, *Fus. Sci. Technol.* **49**, 453 (2006).
2. L. J. Waxer, D. N. Maywar, J. H. Kelly, T. J. Kessler, B. E. Kruschwitz, S. J. Loucks, R. L. McCrory, D. D. Meyerhofer, S. F. B. Morse, C. Stoeckl, and J. D. Zuegel, "High-energy petawatt capability for the Omega laser," *Opt. Photon. News* **16**, 30 (2005).
3. C. P. J. Barty, M. Key, J. Britten, R. Beach, G. Beer, C. Brown, S. Bryan, J. Caird, T. Carlson, J. Dawson, A. C. Erlandson, D. Fittinghoff, M. Hermann, C. Hoaglan, A. Iyer, L. Jones II, I. Jovanovic, A. Komashko, O. Landen, Z. Liao, W. Molander, S. Mitchell, E. Moses, N. Nielsen, H.-H. Ngyuen, J. Nissen, S. Payne, D. Pennington, L. Risinger, M. Rushford, K. Skulina, M. Spaeth, B. Stuart, G. Tietbohl, and B. Wattellier, "An overview of LLNL high-energy short-pulse technology for advanced radiography of laser fusion experiments," *Nucl. Fusion* **44**, S266–S275 (2004).
4. C. Le Blanc, C. Felix, J. C. Lagron, N. Forget, Ph. Hollander, A. M. Sautivet, C. Sauteret, F. Amiranoff, and A. Migus, "The petawatt laser glass chain at LULI: from the diode-pumped front end to the new generation of compact compressors," in *Proceedings of Third International Conference on Inertial Fusion Sciences and Applications*, B. A. Hammel, D. D. Meyerhofer, J. Meyer ter Vehn, and H. Azechi, eds. (American Nuclear Society, 2004), pp. 608–611.
5. C. N. Danson, P. A. Brummitt, R. J. Clarke, J. L. Collier, B. Fell, A. J. Frackiewicz, S. Hancock, S. Hawkes, C. Hernandez-Gomez, P. Holligan, M. H. R. Hutchinson, A. Kidd, W. J. Lester, I. O. Musgrave, D. Neely, D. R. Neville, P. A. Norreys, D. A. Pepler, C. J. Reason, W. Shaikh, T. B. Winstone, R. W. W. Wyatt, and B. E. Wyborn, "Vulcan petawatt–an ultra-high-intensity interaction facility," *Nucl. Fusion* **44**, S239–S246 (2004).
6. N. Blanchot, E. Bignon, H. Coïc, A. Cotel, E. Couturier, G. Deschaseaux, N. Forget, E. Freysz, E. Hugonnot, C. Le Blanc, N. Loustalet, J. Luce, G. Marre, A. Migus, S. Montant, S. Mousset, S. Noailles, J. Néauport, C. Ruyer, C. Rullière, C. Sauteret, L. Videau, and P. Vivini, "Multi-petawatt high energy laser project on the LIL facility in Aquitaine," in *Topical Problems of Non-linear Wave Physics*, A. Sergeev, ed., *Proc. SPIE* **5975**, 30 (2005).
7. K. Mima, H. Azechi, Y. Johzaki, Y. Kitagawa, R. Kodama, Y. Kozaki, N. Miyanaga, K. Nagai, H. Nagatomo, M. Nakai, H. Nishimura, T. Norimatsu, H. Shiraga, K. Tanaka, Y. Izawa, Y. Nakao, and H. Sakagami, "Present status of fast ignition research and prospects of FIREX project," *Fus. Sci. Technol.* **47**, 662 (2005).
8. W. Koechner, "Damage of optical elements," in *Solid-State Laser Engineering*, 5th ed., Vol. 1 of Springer Series in Optical Sciences (Springer-Verlag, 1999), pp. 676–677.
9. M. Born and E. Wolf, *Principle of Optics*, 7th ed. (Cambridge University), p. 186.
10. B. M. Van Wonterghem, S. C. Burkhart, C. A. Haynam, K. R. Manes, C. D. Marshall, J. E. Murray, M. L. Spaeth, D. R. Speck, S. B. Sutton, and P. J. Wegner, "National Ignition Facility commissioning and performance," in *Optical Engineering at the Lawrence Livermore National Laboratory II: The National Ignition Facility*, M. A. Lane and C. R. Wuest, eds., *Proc. SPIE* **5341**, 55–65 (2004).
11. C. Cavailler, N. Fleurot, T. Lonjaret, and J. M. Di-Nicola, "Prospects and progress at LIL and Megajoule," *Plasma Phys. Controlled Fusion* **46**, B135–B141 (2004).
12. Z. Bor, "Distortions of femtosecond laser pulses in lens systems," *J. Mod. Opt.* **35**, 1907–1918 (1988).
13. R. Piestun and D. B. Miller, "Spatiotemporal control of ultrashort optical pulses by refractive-diffractive-dispersive structured optical elements," *Opt. Lett.* **26**, 1373–1375 (2001).

14. U. Fuchs and U. D. Zeitner, "Hybrid optics for focusing ultra-short laser pulses," *Opt. Lett.* **31**, 1516–1518 (2006).
15. T. Stone and N. George, "Hybrid diffractive-refractive lenses and achromats," *Appl. Opt.* **27**, 2960–2971 (1988).
16. H. Madjidi-Zolbanine and C. Froehly, "Holographic correction of both chromatic and spherical aberrations of single glass lenses," *Appl. Opt.* **18**, 2385–2393 (1979).
17. H. M. Heuck, P. Neumayer, T. Köhl, and U. Wittrock, "Chromatic aberration in petawatt-class lasers," *Appl. Phys. B* **84**, 421–428 (2006).
18. T. J. Kessler, H. Huang, and D. Weiner, "Diffractive optics for compensation of axial chromatic aberration in high-energy short-pulse laser," in *Proceedings of the International Conference on Ultrahigh Intensity Lasers* (International Committee on Ultra-High Intensity Lasers, 2006), pp. 126–128.
19. M. L. André, "Status of the LMJ project," in *Solid State Lasers for Applications to Inertial Confinement Fusion: Second Annual International Conference*, M. L. André, ed., Proc. SPIE **3047**, 38 (1997).
20. N. Blanchot, G. Marre, J. Néauport, E. Sibé, C. Rouyer, S. Montant, A. Cotel, C. Le Blanc, and C. Sauteret, "Synthetic aperture compression scheme for multi-petawatt high energy laser," *Appl. Opt.* **45**, 6013–6021 (2006).
21. Z. Bor, "Distortion of femtosecond laser pulses in lenses," *Opt. Lett.* **14**, 119–121 (1989).
22. M. W. Farm and W. B. Veldkamp, "Binary optics," in *Handbook of Optics*, 2nd ed., M. Bass, ed. (McGraw-Hill, 1995), p. 86.
23. V. I. Bespalov and V. I. Talanov, "Filamentary structure of light beams in non-linear liquids," *JETP Lett.* **3**, 307–310 (1966).
24. Schott Optical Glass, Inc., 400 York Avenue, Duryea, Pa. 18642; <http://www.schott.com>.
25. H. Hack and N. Neuroth, "Resistance of optical and colored glasses to 3 ns laser pulses," *Appl. Opt.* **21**, 3239–3248 (1982).
26. R. Adair, L. L. Chase, and S. A. Payne, "Nonlinear refractive index of optical crystals," *Phys. Rev. B* **39**, 3337–3350 (1989).
27. J. H. Campbell, "Damage resistant optical glasses for high power lasers: a continuing glass science and technology challenge," *Glass Sci. Technol.* **75**, 91–108 (2002).
28. M. Martinez, E. Gaul, T. Ditmire, S. Douglas, D. Gorski, W. Henderson, J. Blakeney, D. Hammond, M. Gerity, J. Caird, A. Erlandson, I. Iovanovic, C. Ebberts, and B. Molander, "The Texas Petawatt Laser," in *Laser-Induced Damage in Optical Materials: 2005*, G. J. Exarhos, A. H. Guenther, K. L. Lewis, D. Ristau, M. J. Soileau, and C. J. Stolz, eds., Proc. SPIE **5991**, 1N-1 (2005).
29. M. Bray, A. Liard, and G. Chabassier, "Laser megajoule optics (I): New methods of optical specifications," in *Optical Fabrication and Testing*, R. Geyl and J. Maxwell, eds., Proc. SPIE **3739**, 449–460 (1999).
30. M. Daimon and A. Masumura, "High accuracy measurements of the refractive index and its temperature coefficient of calcium fluoride in a wide wavelength range from 138 to 2326 nm," *Appl. Opt.* **41**, 5275–5281 (2002).
31. CARGILLE Laboratories, Inc., 55 Commerce Road, Cedar Grove, N.J. 07009-1289 USA; <http://www.cargille.com>.
32. <http://www.llnl.gov/nif/last/diffractive-optics/fresnel.html>.